ORIGINAL RESEARCH

Clinical Characteristics and Electrophysiological Mechanisms Underlying Brugada ECG in Patients With Severe Hyperkalemia

Allan Rivera-Juárez MD, PhD;* Ismael Hernández-Romero, MS;* Carolina Puertas, MD; Serena Zhang-Wang, MD; Beatriz Sánchez-Álamo, MD; Raphael Martins MD, PhD; Carlos Figuera, PhD; María S. Guillem, PhD; Andreu M. Climent, PhD; Francisco Fernández-Avilés, MD, PhD; Alberto Tejedor, MD, PhD; José Jalife, MD, FAHA;† Felipe Atienza, MD, PhD, FHRS†

***Background*—**Several metabolic conditions can cause the Brugada ECG pattern, also called Brugada phenotype (BrPh). We aimed to define the clinical characteristics and outcome of BrPh patients and elucidate the mechanisms underlying BrPh attributed to hyperkalemia.

***Methods and Results*—**We prospectively identified patients hospitalized with severe hyperkalemia and ECG diagnosis of BrPh and compared their clinical characteristics and outcome with patients with hyperkalemia but no BrPh ECG. Computer simulations investigated the roles of extracellular potassium increase, fibrosis at the right ventricular outflow tract, and epicardial/endocardial gradients in transient outward current. Over a 6-year period, 15 patients presented severe hyperkalemia with BrPh ECG that was transient and disappeared after normalization of their serum potassium. Most patients were admitted because of various severe medical conditions causing hyperkalemia. Six (40%) patients presented malignant arrhythmias and 6 died during admission. Multiple logistic regression analysis revealed that higher serum potassium levels (odds ratio, 15.8; 95% CI, 3.1–79; P=0.001) and male sex (odds ratio, 17; 95% CI, 1.05–286; P=0.045) were risk factors for developing BrPh ECG in patients with severe hyperkalemia. In simulations, hyperkalemia yielded BrPh by promoting delayed and heterogeneous right ventricular outflow tract activation attributed to elevation of resting potential, reduced availability of inward sodium channel conductance, and increased right ventricular outflow tract fibrosis. An elevated transient outward current gradient contributed to, but was not essential for, the BrPh phenotype.

***Conclusions*—**In patients with severe hyperkalemia, a BrPh ECG is associated with malignant arrhythmias and all-cause mortality secondary to resting potential depolarization, reduced sodium current availability, and fibrosis at the right ventricular outflow tract.
(*J Am Heart Assoc*. 2019;8:e010115. DOI: 10.1161/JAHA.118.010115.)

Key Words: Brugada syndrome • hyperkalemia • Sudden cardiac death

Brugada syndrome (BrS) is characterized by distinctive ST-segment elevation in the right precordial leads of the ECG, and propensity for sudden cardiac death.[1,2] According to the 2013 consensus statement on cardiac arrhythmia syndromes and the 2016 J-Wave syndromes expert consensus conference report, BrS is diagnosed in patients with spontaneous ST-segment elevation (≥2 mm) with type 1 morphology in ≥1 precordial leads, particularly V1 and V2, positioned on the second and third or fourth intercostal spaces.[3,4] BrS has been considered as a primary electric cardiac disease caused by mutations in genes coding sodium, calcium, and potassium channels in ≈30% of patients.[3–5]

From the Department of Cardiology (A.R.-J., I.H.-R., S.Z.-W., B.S.-A., A.M.C., F.F.-A., F.A.), Renal Physiopathology Laboratory, Department of Nephrology (A.T.), and Department of Biochemistry (C.P.), Hospital General Universitario Gregorio Marañón, Instituto de Investigación Sanitaria Gregorio Marañón, Facultad de Medicina, Universidad Complutense, Madrid, Spain; CHU Rennes, Service de Cardiologie et Maladies Vasculaires, Rennes, France (R.M.); Department of Signal Theory and Communications, Universidad Rey Juan Carlos, Madrid, Spain (I.H.-R., C.F.); ITACA, Universitat Politécnica de Valencia, Valencia, Spain (M.S.G., A.M.C.); Center for Arrhythmia Research, University of Michigan, Ann Arbor, MI (J.J.); Departamento de Arritmias Cardíacas, Fundacion Centro Nacional de Investigaciones Cardiovasculares (CNIC), Madrid, Spain (J.J.); CIBERCV, Centro de Investigación Biomédica en Red de Enfermedades Cardiovasculares, Madrid, Spain (A.R.-J., I.H.-R., A.M.C., F.F.-A., J.J., F.A.).

*Dr Rivera-Juárez and Dr Hernández-Romero contributed equally to this work as co-first authors.

†Dr Jalife and Dr Atienza contributed equally to this work as co-senior authors.

Correspondence to: Felipe Atienza, MD, PhD, Cardiology Department, Hospital General Universitario Gregorio Marañón, C/Dr Esquerdo, 46, 28007 Madrid, Spain. E-mail: fatienzaf@secardiologia.es

Received June 19, 2018; accepted December 7, 2018.

Clinical Perspective

What Is New?

- In patients with severe hyperkalemia resulting from a critical medical condition, the presence of a Brugada syndrome ECG phenotype is associated with a high prevalence of malignant arrhythmias and all-cause mortality.
- Higher serum potassium levels and male sex are independent predictors for the presence of a Brugada ECG phenotype.
- Modeling studies indicate that the Brugada ECG phenotype induced by severe hyperkalemia occurs secondary to membrane depolarization and consequent reduced sodium channel availability, resulting in delayed and heterogeneous conduction, particularly in the presence of fibrosis at the right ventricular outflow tract.

What Are the Clinical Implications?

- Prompt recognition of this clinical-morphological entity and immediate treatment of hyperkalemia and surveillance of potential life-threatening arrhythmias is strongly recommended.
- Drug-provocation testing following normalization of serum potassium levels may be considered to uncover underlying Brugada syndrome.

However, other studies found no clear genetic association, and minor structural abnormalities were associated with the syndrome.[6–8] Moreover, some environmental factors can induce ECG morphologies similar or identical to BrS in the absence of genetic mutations or ion-channel dysfunction.[6,9] The acquired form of Brugada-like ECG pattern, also called Brugada phenotype (BrPh), is manifested by a Brugada ECG pattern in the presence of an identifiable underlying condition and typically disappears after its resolution.[3,4,10–12] Multiple metabolic conditions can lead to BrPh ECG; the majority of cases are associated with serum K^+ abnormalities, hyperkalemia being the most frequent single cause.[10] Although classical hyperkalemia produces several well-described ECG alterations, only a minority of patients develop BrPh.[10,12] Nevertheless, the clinical characteristics and prognostic impact on patients developing BrPh are poorly known.

The main mechanism responsible for BrS phenotype relate to abnormal patterns of repolarization and/or impulse activation at the right ventricular outflow tract (RVOT).[13–16] However, whether BrPh represents transient alterations in myocardial depolarization, repolarization, or any other mechanism is yet to be elucidated. Moreover, the transient nature of BrPh casts doubt about its genetic origin or relation to structural abnormalities, or both.

The objectives of the study were several fold, including to: (1) describe the clinical and ECG characteristics and clinical outcome of patients with hyperkalemic BrPh; (2) compare the clinical characteristics of patients with hyperkalemic BrPh with those of patients with severe hyperkalemia but no BrPh ECG; (3) conduct computer simulations in a three-dimensional model of ventricular propagation under conditions of varying hyperkalemia to analyze the implication of mutations and/or structural abnormalities in relation to the Brugada sign[17]; (4) study the mechanisms underlying hyperkalemic BrPh; and (5) evaluate the proarrhythmic risk of BrPh in the presence of hyperkalemia.

Methods

Data, analytical methods, and study materials will be made available to other researchers for purposes of reproducing the results or replicating the procedure. The data will be made available for requests made to corresponding author by e-mail.

Patients

From 2010 to 2016, we prospectively identified patients hospitalized at our institution who presented an ECG suggestive of BrS in the context of severe hyperkalemia (group 1). Inclusion in this series required moderate-to-severe hyperkalemia (serum potassium [K^+] $\geq$6.5 mmol/L), hospitalization for an acute illness and type 1 or 2 Brugada ECG pattern on right precordial leads V1 to V2, which normalized after serum K^+ levels returned to reference values.[10] Additionally, we also considered patients with atypical ST-segment elevation on the right precordial leads without BrS and/or aVR sign.[18,19] Furthermore, we retrospectively reviewed the charts of all adults admitted to our center during 2013 who developed severe hyperkalemia any time during admission, with an available ECG recording at peak serum K^+ $\geq$6.5 mmol/L (group 2).

For all patients, we recorded demographic and clinical characteristics, laboratory data, treatments, and hospital outcomes, including diagnosis at discharge and survival status. The ECGs obtained during peak serum K^+ were analyzed for rate, rhythm, *P*-wave voltage, PR interval duration, QRS width, QRS axis, QTc interval, maximum height of ST-segment elevation, and T wave height. In group 1 patients, the recorded ECGs were compared before and after treatment of hyperkalemia. In group 1 patients displaying a BrPh ECG, a provocative flecainide test was performed after normalization of the electrolyte disturbances. Patients were considered to be at a low clinical probability of having BrS if they had a negative flecainide challenge test, a lack of family history of syncope or sudden death, no previous history of syncope or cardiac arrhythmia, and normal body temperature.[10] The institutional review board of our center waived the informed consent form and approved the study.

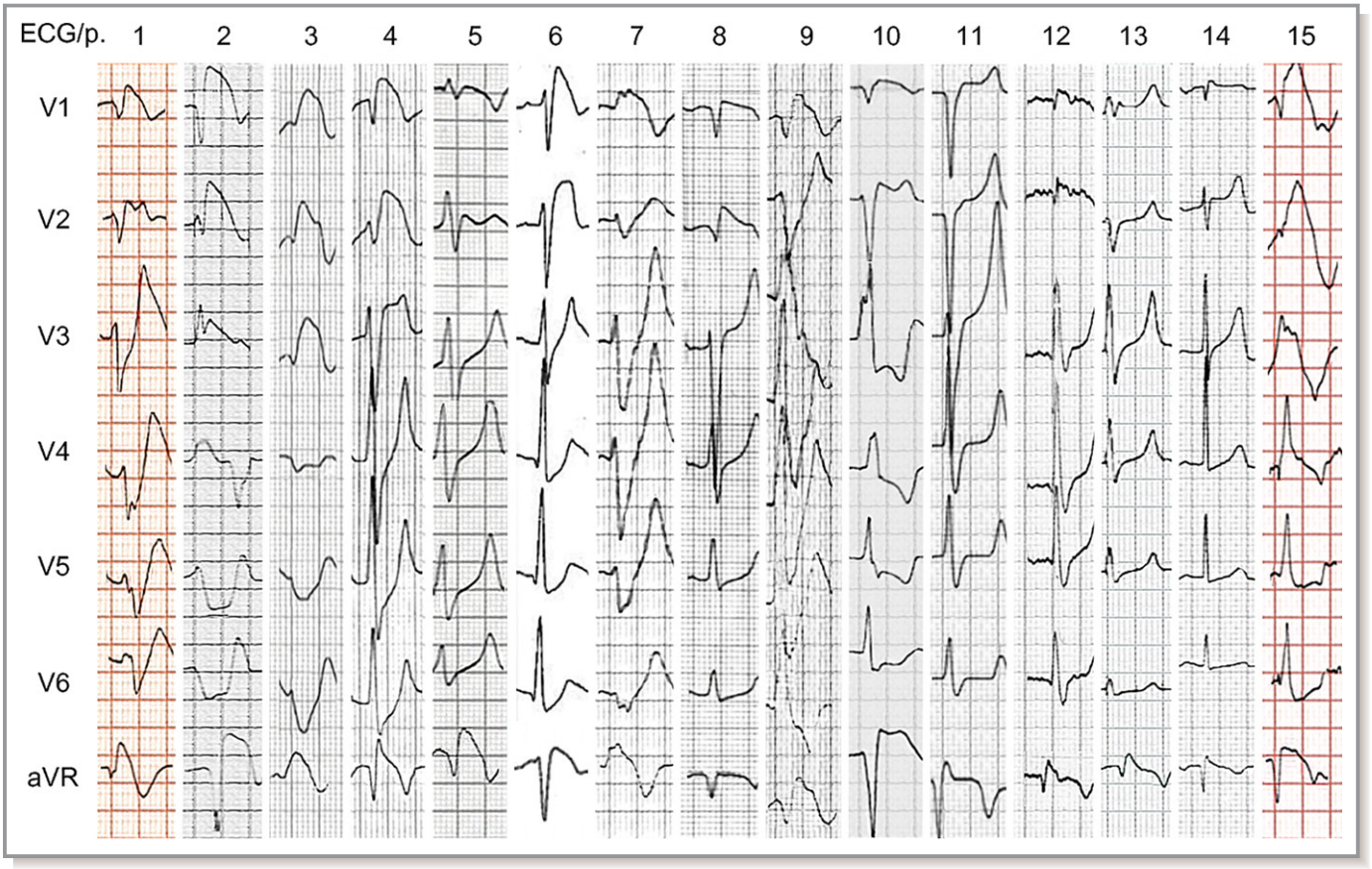

Figure 1. ECG recordings of patients displaying brugada ECG pattern at the time of peak hyperkalemia (precordial and aVR leads).

Computer Simulations

A multiscale computer model was constructed to determine conditions for the BrPh ECG in patients with hyperkalemia. The model was based on several parameters, including electrophysiological dynamics, transmural differences in cell type, fiber orientation, and fibrosis at varying extracellular potassium concentrations ([K+]o) ranging between 5.4 and 10.5 mmol/L. A human wedge model of the anterior ventricular wall, including both ventricles and the RVOT, was created using a reference geometry (normal young male), available for the ECGSIM software.[20] The mesh contained 281 191 nodes and 1 460 832 elements with a mean edge length of 290.8±296.6 μm. Human ventricular cell dynamics and action potential morphologies of cell types were simulated using the O'Hara–Rudy model,[21] with modifications in the sodium current suggested by Dutta et al,[22] which enabled realistic simulations under hyperkalemic conditions. Ventricular activation sequences were based on Cardone-Noott et al,[23] being initiated in 3 areas in our model. Anisotropic conduction attributed to fiber orientation changes was incorporated into the model using an anisotropy ratio of 10:1, D||:D⊥, where D|| and D⊥ are the longitudinal and transverse diffusion coefficients, respectively. Therefore, propagation in any direction of the three-dimensional model depended on fiber direction. The RVOT diffusion coefficient was 25% of either ventricle, keeping the same anisotropy ratio.

Simulations were performed under 4 different conditions: (1) healthy RVOT; (2) fibrotic RVOT; (3) RVOT with a gradient of transient outward potassium current (I_{to}); and (4) fibrotic RVOT with an epi- to endocardium I_{to} gradient. Various $[K^+]_o$ concentrations (5.4, 7.5, 10.0, and 10.5 mmol/L) were chosen considering that the level of serum K^+ registered in patients could be lower than in the extracellular space.[24] Different $[K^+]_o$ were tested in basal conditions and RVOT with 65% of fibrotic tissue. Fibrotic tissue was modeled by randomly disconnecting a specific percentage of available nodes in the RVOT. The enhanced I_{to} conductance gradient was established by increasing the maximal conductance of the current on the epicardium of the RVOT, from its basal level (0.08 mS/μF) to 0.30, 0.70, and 1.50 mS/μF; these values were consistent with experimentally derived data related to BrS.[25] Different cases were tested, combining the amount of fibrosis (55, 65, and 75%), $[K^+]_o$ concentrations (5.4 and

Table 1. Clinical Characteristics and Outcome of Patients With Brugada Phenotype

Pt	Sex	Age, y	K^+ (mmol/L)	Hospital Admission Reason	Hyperkalemia Etiology	Flecainide Test	Diagnosis	Outcome
1	F	62	8.2	OH SCD	Potassium supplements overdose	No	Suicide	Death
2	M	89	7.4	Diarrhea dehydration	CKD descompensation	No*	Gastrointestinal infection	Alive
3	M	45	7.7	Decompensated liver cirrhosis	AKD	No	Terminal liver disease	Death, 3 months after discharge
4	M	53	6.9	DKA	AKD	Yes	DKA, BrS	Alive
5	F	83	9.1	OH SCD	≥2 RAAS inhibitors	No	Hyperkalemia	Death
6	M	63	8.6	Sepsis	AKD Espironolactone	No	Bilateral pneumonia	Death
7	M	41	7.7	OH SCD	AKD	No	Benzodiazepine overdose	Death
8	M	38	7.2	Dehydration	AKD	Yes	Gastrointestinal infection	Alive
9	F	57	8.6	Sepsis	AKD	No	Urinary tract infectionadvanced breast cancer	Death
10	M	61	6.8	Lung cancer surgery	IV fluid overdose	Yes	Lung cancer	Alive
11	M	78	8.5	Diarrhea dehydration	AKD	Yes	Gastrointestinal infection	Alive
12	M	54	7.5	Acute renal disease	AKD	No*	Gastrointestinal infection	Alive
13	M	35	8.1	Abdominal cancer	AKD	No	Metastatic testicular cancer	Death
14	M	41	8.6	Sepsis	CKD	No*	Sepsis	Alive
15	M	46	7.7	DKA	AKD	Yes	DKA	Alive

≥2 RAAS inhibitors indicates combination of ≥2 ACE inhibitor, angiotensin II–receptor blocker, aldosterone antagonist, or renin inhibitors; AKD, acute kidney disease; BrS, Brugada syndrome; CKD, chronic kidney disease; DKA, diabetic ketoacidosis; OH SCD, out-of-hospital sudden cardiac death.
*Flecainide test not performed because of clinical reasons or living overseas.

10.5 mmol/L), and increasing I_{to} conductance gradient from baseline to the maximal conductance, 1.50 mS/μF. Monodomain equations were solved using the Forward-Euler algorithm with a fixed time step of 0.01 ms on a graphic processors unit (GPU Tesla K20 5GRAM DDR5).[26] Three virtual electrodes were positioned at standard electrode locations for the calculation of pseudo-ECGs V1, V2, and V3.

Statistical Analyses

Categorical variables are reported as number and percentage and were compared using Fisher's exact test or the chi-square test, as appropriate. For continuous variables, normal distribution was assessed by the Kolmogorov–Smirnov test and are reported as mean±SD or median and interquartile range, depending on whether they were normally or non-normally distributed. Continuous variables comparisons were made using the Student *t* test or nonparametric tests, as appropriate. Multiple logistic regression analysis was performed to identify predictors of a BrPh ECG in patients with severe hyperkalemia. Analyses were performed using SPSS software (version 22; SPSS, Inc, Chicago, IL), and statistical significance was established at $P<0.05$.

Results

Clinical Characteristics and Outcome of Patients With Hyperkalemic BrPh

During a 6-year observation period, we identified 15 patients with severe hyperkalemia and type 1 or 2 ECG Brugada pattern or atypical repolarization signs on the right precordial leads (ST-segment elevation on the right precordial leads pattern).[3,4,18] Figure 1 shows ECG data from precordial lead recordings from each patient displaying a BrPh ECG at the time of peak hyperkalemia. None of the patients had a family history of BrS, cardiac arrhythmias, or syncope. Baseline clinical characteristics, hospital admission reason, and etiology of hyperkalemia are shown in Table 1. In all cases, ECG changes were transient and disappeared after plasma serum K^+ levels returned to normal (Table 2).

Most patients were middle aged (56.4±16 years old) men (79%), presenting a critically ill state on admission. In fact, 3 were brought to the emergency room because of out-of-hospital sudden cardiac arrest. The most frequent primary etiology of hyperkalemia was decompensated renal function. Six (43%) patients died during admission for different reasons (Table 1): Two patients presented postanoxic encephalopathy,

Table 2. Electrocardiographic Characteristics at Peak K^+ Levels and Following K^+ Levels Normalization in Patients Displaying a Brugada ECG Pattern Recording

	ECG at Peak Hyperkalemia Brugada Phenotype (n=15)	ECG After K levels Normalization (n=15)	*P* Value
Heart rate, bpm, median (IQR)	89 (26)	60 (60–89)	0.08
P-wave voltage, mm, median (IQR)	0.5 (0.5–1)	1 (0.5–1.3)	0.13
PR segment, ms, median (IQR)	160 (160–220)	160 (130–190)	0.27
QRS abnormal axis, n (%)	9 (60)	2 (16)	0.04
QRS width, ms, median (IQR)	120 (110–160)	80 (80–120)	0.001
QTc segment, ms, median (IQR)	433 (69)	420 (395–430)	0.58
T wave height, mm, median (IQR)	7 (5–14)	3 (3–6)	0.002

IQR indicates interquartile range; K, potassium.

1 had recurrent cardiac arrest at the time of arrival in the emergency room, and 2 presented septic shock (patients 6 and 9). One patient died after prolonged admission because of metastatic testicular cancer. Patient 3 died 3 months after hospital discharge because of terminal hepatic disease.

We contacted 8 of the surviving patients, and a flecainide test was finally performed in 5 (of the other 3, 1 was dismissed because of severe neurologic chronic sequelae and 2 lived overseas). The flecainide test was negative in 4 patients and positive in 1. Patient 4 was a 53-year-old male admitted for diabetic ketoacidosis with hyperkalemia (K^+, 6.9 mmol/L; serum pH, 6.89). He presented a BrPh pattern on admission (Figure 2A), which was normalized after correction of the serum K^+ (4.5 mmol/L; serum pH, 7.1; Figure 2B). Several weeks after hospital discharge, while the patient was clinically stable, a flecainide test (2-mg/kg intravenous infusion over 10 minutes) uncovered a type 1 Brugada pattern (Figure 2C).

Clinical Characteristics and Outcome of Patients With Hyperkalemic BrPh Versus Severe Hyperkalemia With Non-BrPh Pattern

During 2013, 245 patients presented severe hyperkalemia of 46 459 admitted to our institution (0.53%). Of those, 44 (18%) had an ECG recording available at the time of peak hyperkalemia. Table 3 shows baseline characteristics of BrPh patients (group 1) and severe hyperkalemic patients without BrPh (group 2). Compared with group 2 patients, BrPh patients were younger and had higher serum K^+ values (1 mmol/L higher on average), lower pH, and less chronic kidney disease; hypertension tended to be less prevalent and so was the use of angiotensin-receptor blockers. On ECG, BrPh hyperkalemic patients showed wider QRS, and frequently presented abnormal QRS axis and greater T-wave height compared with non-BrPh hyperkalemic patients (Table 3). Multivariate analysis

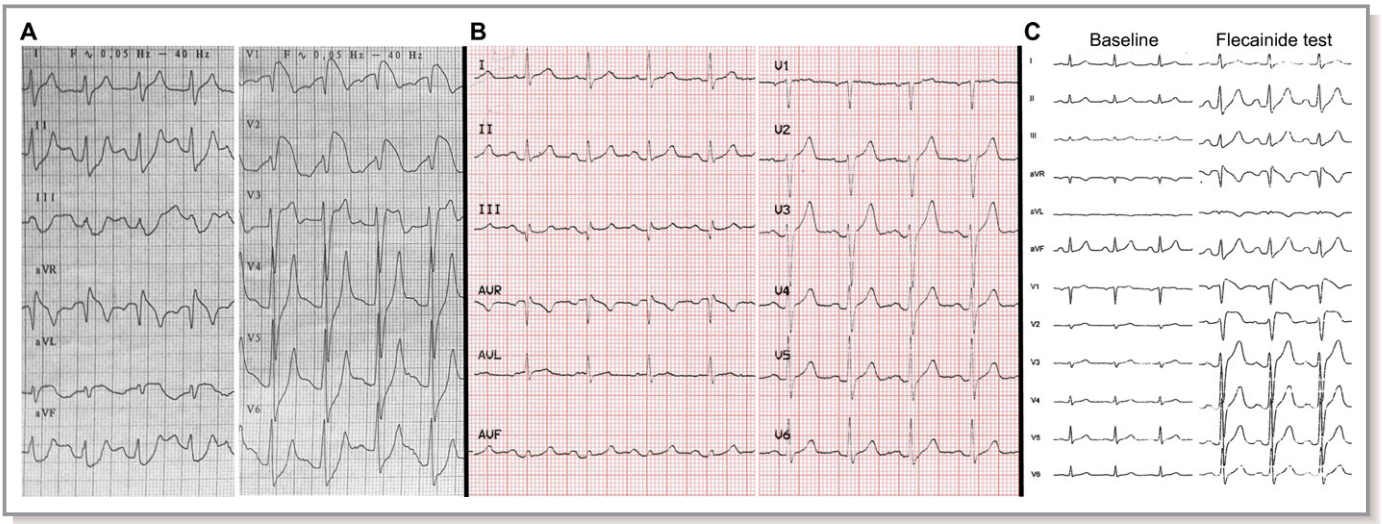

Figure 2. Brugada pattern uncovered by hyperkalemia in a patient with Brugada syndrome. **A**, Patient previously asymptomatic, admitted because of diabetic ketoacidosis, displaying an ECG Brugada pattern. **B**, ECG normalized after correction of the electrolyte disturbances. **C**, Baseline ECG and following infusion of Flecainide.

Table 3. Clinical Characteristics in Patients With (Group 1) Versus Without Brugada Phenotype Pattern (Group 2) in the Presence of Severe Hyperkalemia

Clinical Characteristics and Outcome	Group 1 Hyperkalemic Brugada Phenotype (n=15)	Group 2 Hyperkalemic Non-Brugada Phenotype (n=44)	*P* Value
Age, y, median (IQR)	54 (41–62)	74 (60–83)	0.002
Female, n (%)	3 (20)	20 (46)	0.08
Hypertension, n (%)	7 (47)	31 (71)	0.06
Diabetes mellitus, n (%)	7 (47)	20 (45)	0.94
CKD, n (%)	3 (20)	23 (52)	0.04
Smoking, n (%)	4 (27)	12 (27)	0.92
Cardiac disease, n (%)	5 (33)	26 (59)	0.12
COPD, n (%)	1 (7)	11 (25)	0.15
BB, n (%)	3 (20)	17 (39)	0.19
ACE inhibitor, n (%)	5 (33)	9 (21)	0.53
ARB, n (%)	0	8 (18)	0.09
Mineralocorticoid antagonist, n (%)	3 (20)	6 (14)	0.48
Glycemia, mmol/L, median (IQR)	144 (101–272)	131 (105–185)	0.52
Crp, mg/dL, median (IQR)	3.2 (1.7–12.4)	2.5 (1.5–3.8)	0.31
(K), mmol/L, median (IQR)	7.7 (7.4–8.6)	6.9 (6.6–7.2)	<0.001
Serum sodium, mmol/L, median (IQR)	132 (115–136)	133 (130–136)	0.12
Serum pH, median (IQR)*	7.07 (6.9–7.2)	7.25 (7.2–7.3)	0.003
HCO_3, mEq/L, median (IQR)*	16 (5–20)	20 (15–27)	0.03
LVEF<60%, n (%)	0	11 (36)	0.03
Exitus, n (%)	6 (40)	18 (43)	0.85

ACE inhibitor indicates angiotensin-converting-enzyme use; ARB, angiotensin-receptor blocker use; BB, betablocking agent; CKD, chronic kidney disease; COPD, chronic obstructive pulmonary disease; IQR, interquartile range; LVEF, left ventricular ejection fraction.
*Available in 49 patients.

revealed that higher serum K^+ levels (odds ratio, 15.8; 95% CI, 3.1–79; *P*=0.001) and male sex (odds ratio, 17; 95% CI, 1.05–286; *P*=0.045) were independent predictors for developing BrPh ECG in patients with severe hyperkalemia. Moreover, lower arterial pH, available in a smaller number of patient samples, was also related to development of BrPh ECG (Tables 3 and 4).

Of 15 patients with BrPh, 6 (40%) had malignant arrhythmias (3 presented as sudden cardiac arrest): 4 had ventricular tachycardia, 1 ventricular fibrillation, and 1 high-degree atrioventricular block. In group 2, 11 patients (25%) had malignant arrhythmias: 7 high-degree atrioventricular block, 3 ventricular tachycardia, and 1 ventricular fibrillation. Thus, patients with BrPh had a higher likelihood of developing

Table 4. Electrocardiographic Characteristics in Patients With Versus Without Brugada Phenotype Pattern

	Group 1 Hyperkalemic Brugada Phenotype (n=15)	Group 2 Hyperkalemic Non-Brugada Phenotype (n=44)	*P* Value
Heart rate, bpm, median (IQR)	87 (75–115)	80 (63–99)	0.20
P-wave voltage, mm, median (IQR)	0.5 (0.4–1.3)	0.5 (0.5–1.0)	0.67
PR segment, ms, median (IQR)	160 (160–210)	160 (120–180)	0.32
QRS abnormal axis, n (%)	8 (57.1)	17 (38.6)	0.01
QRS width, ms, median (IQR)	130 (110–160)	100 (80–120)	0.03
QTc segment, ms, median (IQR)	425 (368–475)	415 (390–450)	0.68
T-wave height, mm, median (IQR)	7.5 (5.4–14.5)	4 (2.5–6.0)	0.001

IQR indicates interquartile range.

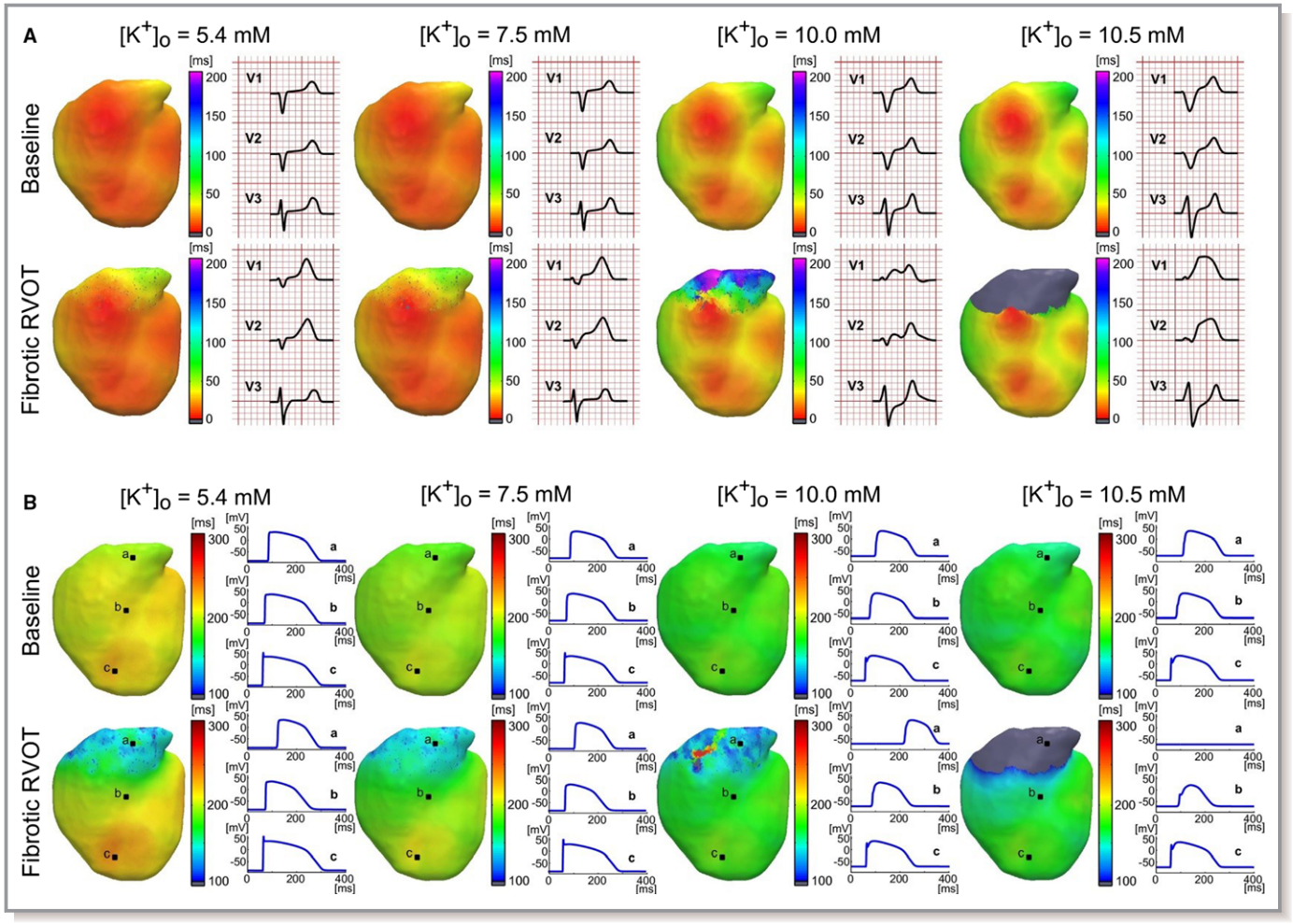

Figure 3. Computer simulations testing the role of fibrosis of the right ventricular outflow tract (RVOT) at different levels of hyperkalemia. A, Activation isochrones maps of the anterior wall with healthy (upper) and fibrotic RVOT (bottom), under basal conditions with extracellular potassium concentration ($[K^+]_o$)=5.4 mmol/L and hyperkalemic conditions with $[K^+]_o$=7.5 mmol/L, $[K^+]_o$=10.0 mmol/L, and $[K^+]_o$=10.5 mmol/L. Pseudo-ECGs of V1, V2, and V3 leads are shown in each case. **B**, Action potential duration (APD) maps and corresponding action potential signals of sites a, b, and c are shown in each case.

malignant arrhythmias. Nevertheless, total in-hospital mortality was similar (P<0.9) in both groups: 6 patients in group 1 (43%) versus 18 patients in group 2 (41%).

Hyperkalemia, Fibrosis, and the Mechanism of BrPh

To differentiate between the mechanisms underlying BrPh versus non-Brugada ECGs during hyperkalemia, we simulated the effects of increasing $[K^+]_o$ in a human wedge model of the anterior ventricular walls, including the RVOT. Elevating the $[K^+]_o$ reduced the resting membrane potential throughout from −87.9±0.1 mV at $[K^+]_o$=5.4 mmol/L to −69.93±0.08 mV at $[K^+]_o$=10.5 mmol/L, regardless of whether or not the RVOT was fibrotic. As expected, the depolarized resting potential reduced the availability of the sodium channels and slowed the conduction velocity (CV). Figure 3A shows activation sequences and V1 to V3 recordings for 4 different $[K^+]_o$ (5.4, 7.5, 10.0, and 10.5 mmol/L) in the presence and absence of fibrosis at the RVOT. Conduction at the RVOT was significantly altered at 65% fibrosis, with changes in the activation sequence that promoted the appearance of late and fractionated potentials on V1 to V3. There was a progressive slowing of conduction with increasing $[K^+]_o$. At 5.4 mmol/L, CV at the RVOT in the absence of fibrosis was 97.89 versus 60.81 cm/s when fibrosis was included. In hyperkalemic conditions ($[K^+]_o$=10.0 mmol/L), CV was 57.53 cm/s at baseline versus 28.66 cm/s in the fibrotic RVOT. Increasing $[K^+]_o$ to 10.5 mmol/L reduced CV to 47.22 cm/s at baseline, but produced unexcitability and propagation failure in the fibrotic RVOT. A similar progression was also apparent on the V1, V2, and V3 recordings for each $[K^+]_o$ and normal/fibrotic state. Notable changes occurred on leads V1 and V2, where there was delayed activation at the

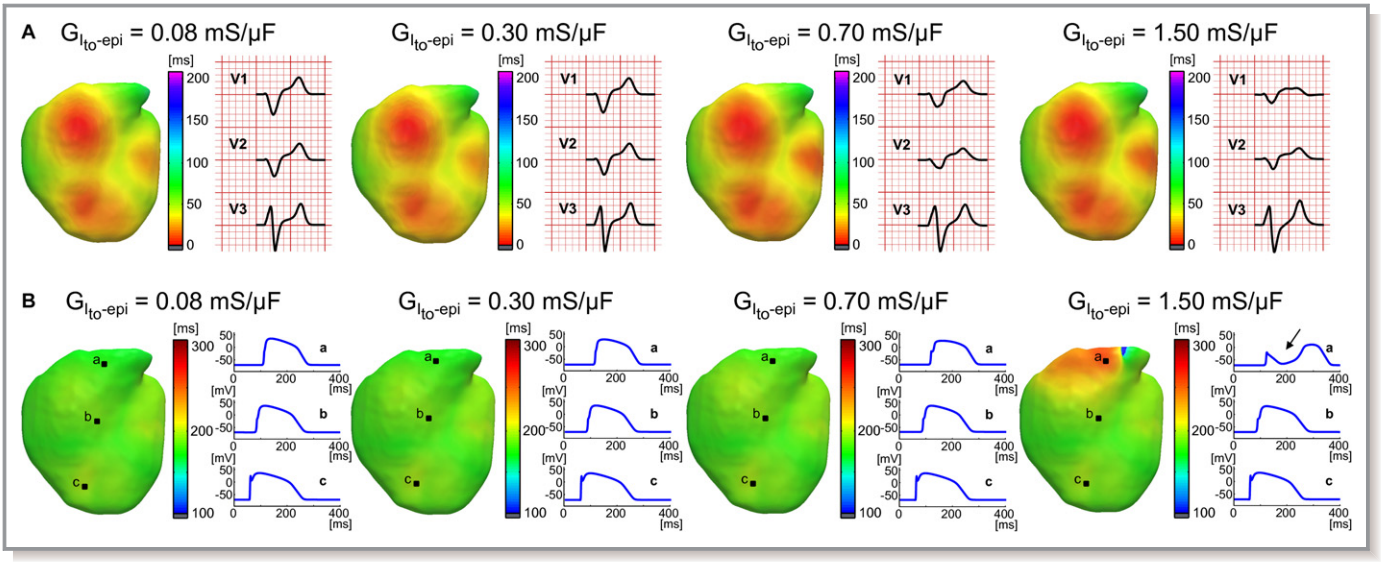

Figure 4. Computer simulations testing the role of incremental transient outward current (I_{to}) conductance. **A**, Activation isochrones maps of the anterior right ventricular outflow tract (RVOT) wall with increasing the maximal conductance of I_{to} in the RVOT epicardium, from its basal level to a characteristic value in BrS modeling (from 0.08 to 1.50 mS/μF, showing 0.30 and 0.70 mS/μF), under severe hyperkalemia (extracellular potassium concentration $[K^+]_o$=10.5 mmol/L). Pseudo-ECGs of V1, V2, and V3 leads are shown in each case. **B**, Action potential duration (APD) maps and corresponding action potential signals of sites a, b, and c are shown in each case. BrS indicates Brugada syndrome.

RVOT, which prolonged the QRS interval proportionately. Moreover, the ST-segment elevated and gradually fussed with the T wave as the $[K^+]_o$ increased. In the absence of fibrosis, at $[K^+]_o$=10.0 mmol/L, the model reproduced the characteristic features of hyperkalemia in patients with healthy RVOT. In contrast, in the fibrotic case, conduction slowing or block promoted ST-segment elevation on V1 and V2, consistent with the classical BrS descriptors. In Figure 3B, the corresponding action potential duration (APD) maps show a progressive global decrease in the APD as $[K^+]_o$ is increased. As illustrated also by the action potential recordings at specific locations, fibrosis intensified both the APD shortening and the activation delay at the RVOT and its immediate vicinity.

Role of I_{to}

Previous evidence has implicated the epicardial-to-endocardial I_{to} gradient within the right ventricle in the pathogenesis and phenotypic expression of BrS.[2] We therefore conducted additional simulations to test the consequences of combining hyperkalemia with increased epicardial I_{to} gradient at the RVOT in the presence and absence of fibrosis. The gradient was established by increasing the baseline value of the epicardial band to 0.30, 0.70, and 1.50 mS/μF, while leaving the endocardium at the basal level (0.08 mS/μF). In Figure 4A, under basal $[K^+]_o$ conditions, we had to increase the maximal I_{to} conductance up to 1.50 mS/μF, to enable BrPh, a value that is characteristic of BrS modeling.[4] Increasing I_{to} produced a progressively exaggerated action potential notch (arrow) at the RVOT while the rest of the tissue was undergoing initial depolarization during the plateau (Figure 4B). On the electrograms, these events coincided with ST-segment elevation (Figure 4A).

As illustrated in Figure 5, the combined effects of fibrosis, elevated $[K^+]_o$-induced membrane depolarization leading to reduced excitability, and increased I_{to} density greatly facilitated the appearance of BrPh on leads V1 to V2. In Figure 5A, a BrPh pattern was already evident on V1 and V2 at 55% fibrosis even when the epicardial I_{to} was at baseline (0.08 mS/μF). The effect was even greater when fibrosis at the RVOT was increased to 75%. Here, ST-segment elevation occurred at 10 mmol/L $[K^+]_o$ because of extreme conduction delay at the RVOT (Figure 5B).

In additional simulations, we assessed the effects of fibrosis and I_{to} current gradient on the entire ventricular wall. The effects were similar to those observed when such changes were only applied to the RVOT. The relative increase in I_{to} over the entire epicardial surface with respect to the endocardium simulated characteristics of the Brugada pattern (Figure 6). At baseline, the I_{to} gradient caused an increase in the duration of the epicardial action potential by increasing the transmembrane potassium outflow during the whole plateau phase. This slightly elevated the ST segment and decreased the T-wave amplitude, even depressing the T wave on V3. However, the $[K^+]_o$ increase also depolarized the membrane potential and reduced the availability of the sodium channels. Consequently, conduction velocity was reduced and the APD was abbreviated, with the appearance of regions of activation failure. Fibrosis throughout the ventricular surface slowed activation and

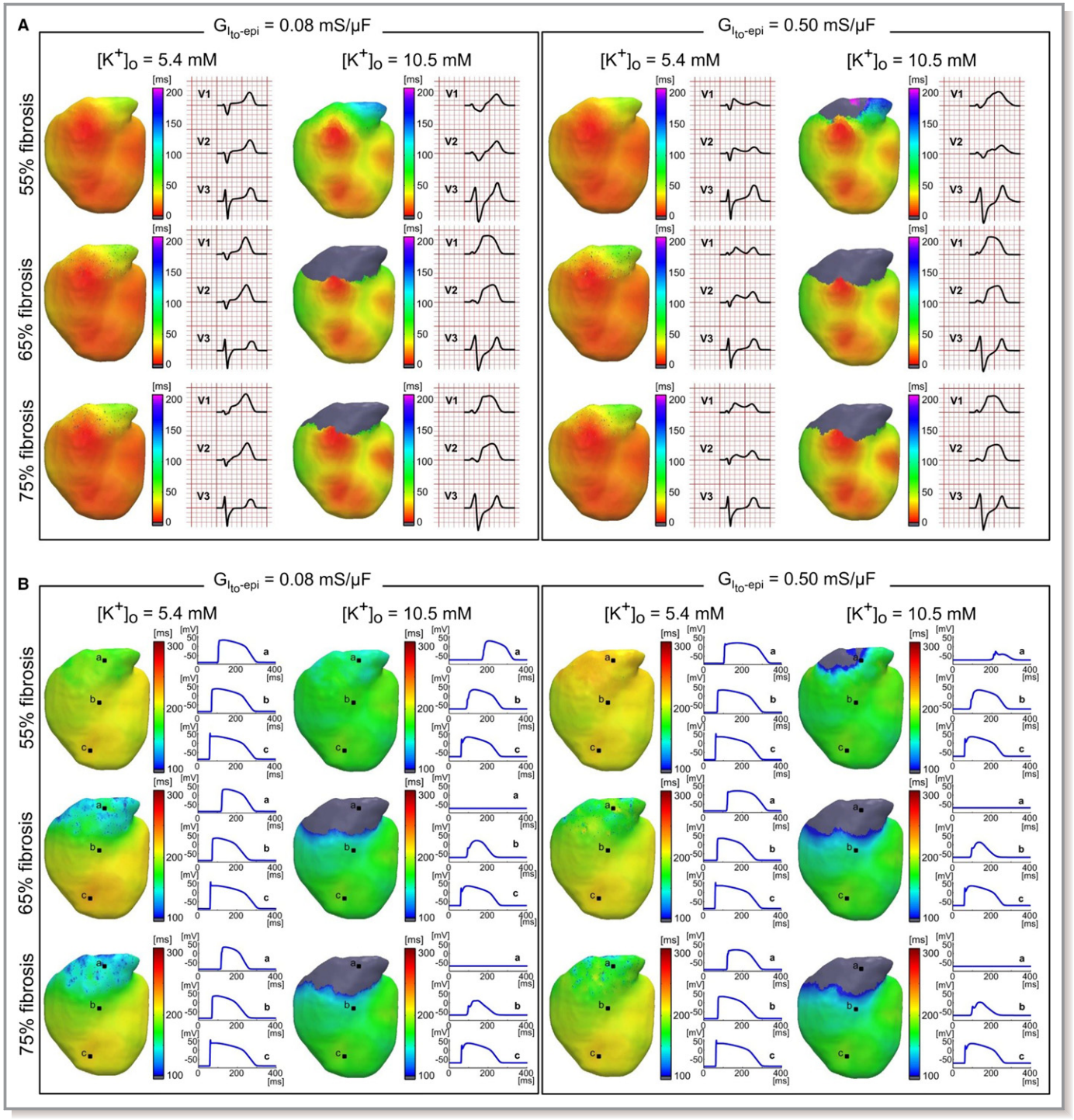

Figure 5. Computer simulations testing the role of incremental fibrosis, transient outward current (I_{to}) conductance, and extracellular potassium concentration ($[K^+]_o$) conditions. **A**, Activation isochrones maps of the anterior right ventricular outflow tract (RVOT) wall with different degrees of fibrosis (55, 65, and 75%), at baseline and severe $[K^+]_o$ concentrations (5.4 and 10.5 mmol/L, respectively), combined with 2 values of maximal conductance of I_{to}: basal (0.08 mS/μF) or increased (0.50 mS/μF). Pseudo-ECGs of V1, V2, and V3 leads are shown in each case. **B**, Action potential duration (APD) maps and corresponding action potential signals of sites a, b, and c are shown in each case.

wavefront propagation (Figure 7), prolonging the QRS and delaying T-wave activation more than when fibrosis was present in the RVOT. When the $[K^+]_o$ was raised to a pathological threshold, conduction slowed further with propagation failure in areas with less excitable cardiac tissue, including the RVOT and its surroundings. ST-segment elevation did not occur under these conditions because of the conduction slowing generated.

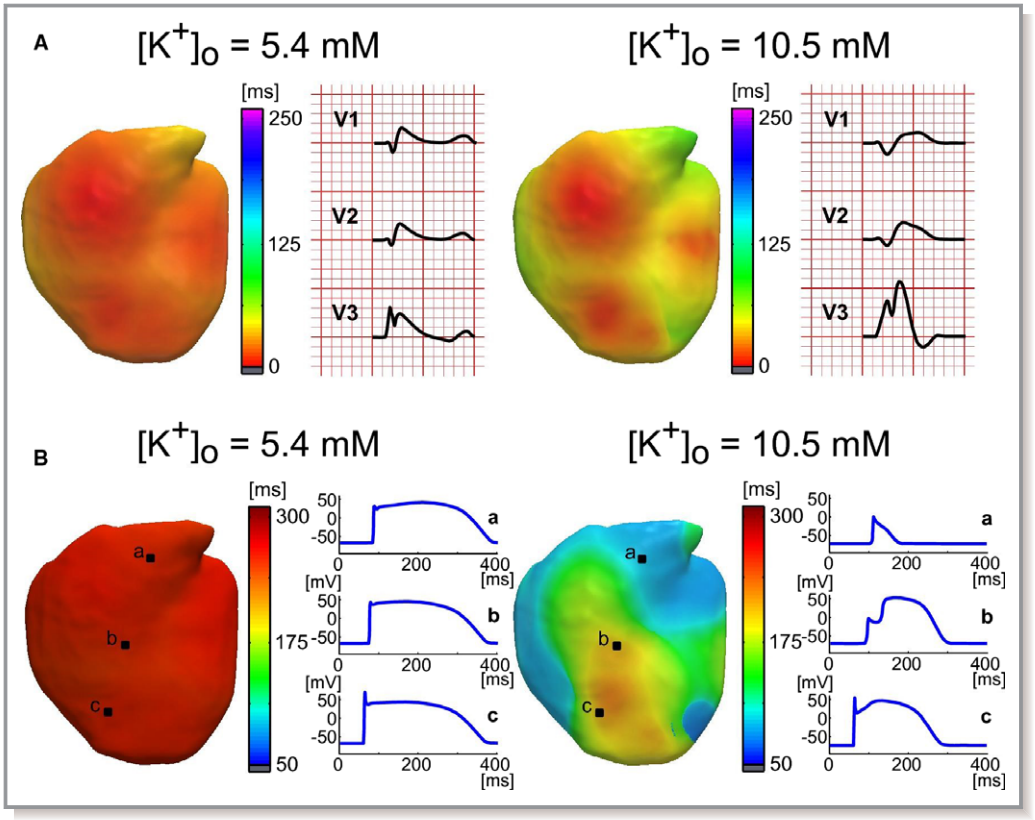

Figure 6. Computer simulations testing the role of gradient of I_{to} conductance over the entire epicardial surface at different levels of extracellular potassium concentration ($[K^+]_o$). **A**, Activation isochrones maps with I_{to} maximal conductance in the whole epicardium to a characteristic value in BrS modeling (1.50 mS/μF), under basal conditions ($[K^+]_o$=5.4 mmol/L) and hyperkalemic conditions ($[K^+]_o$=10.5 mmol/L). Pseudo-ECGs of V1, V2, and V3 leads are shown in each case. **B**, Action potential duration (APD) maps and corresponding action potential signals of sites a, b, and c are shown in each case. BrS indicates Brugada syndrome; I_{to}, transient outward current.

Proarrhythmic Risk of BrPh Pattern Attributed to Hyperkalemia

The foregoing simulations provide insight into the mechanism underlying the observed predisposition of BrPh patients to malignant arrhythmias, as illustrated in the following clinical example: Patient 5 (Table 1) arrived at the emergency department after suffering an out-of-hospital sudden death episode, showing complex ventricular rhythm with wide QRS. An intravenous bolus of adenosine (12 mg) transiently slowed the rhythm and normalized the QRS complex duration. When the adenosine effect faded, the ventricular rhythm accelerated and resumed with progressive QRS widening (Figure 8A through 8C). The patient had a low conscience level, was tachypneic, and had a blood pressure of 100/55 mm Hg. Urgent blood analyses showed serum K^+ levels of 9.1 mmol/L. He was treated with intravenous fluids (2 L of glucosaline), intravenous sodium bicarbonate, 1 g of intravenous calcium chloride, and insulin. One hour later, the K^+ level was 8.1 mmol/L and the ECG showed a BrPh pattern (Figure 8C). The observed changes were consistent with adenosine activation of $I_{K,Ado}$ channels, which, by increasing K^+ conductance, hyperpolarized the cell membrane, abbreviated the APD and the refractory period, and inhibited spontaneous pacemaker discharge, leading to significant QRS narrowing and transient sinus arrest.[27] This finding was further confirmed by our computer simulations. In Figure 9, we used a fibrotic RVOT with hyperkalemic conditions at $[K^+]_o$=10.0 mmol/L. A burst stimulus train with an extra stimulus at 400 ms increased electrogram fractionation and caused unidirectional block that allowed stable reentry formation at the RVOT.

Discussion

The main findings of this study are as follows: 1. In patients with severe hyperkalemia resulting from a critical medical condition, the presence of a BrS phenotype is associated with a high prevalence of malignant arrhythmias and all-cause mortality. 2. In surviving patients, the characteristic Brugada ECG changes are transient and disappear when the serum K^+ levels normalize. 3. In patients with BrS, hyperkalemia may elicit the typical BrS ECG manifestations. 4. Higher serum K^+

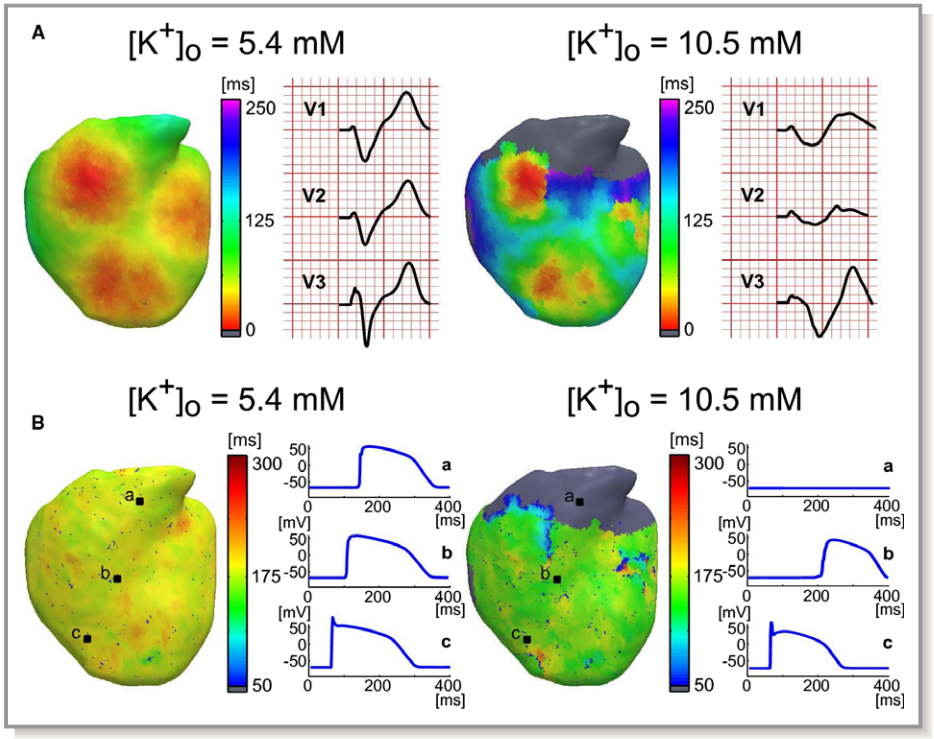

Figure 7. Computer simulations testing the role of fibrosis over the entire epicardial surface at different levels of extracellular potassium concentration ($[K^+]_o$). **A**, Activation isochrones maps with fibrosis in the whole (65%), under basal conditions ($[K^+]_o$=5.4 mmol/L) and hyperkalemic conditions ($[K^+]_o$=10.5 mmol/L). Pseudo-ECGs of V1, V2, and V3 leads are shown in each case. **B**, Action potential duration (APD) maps and corresponding action potential signals of sites a, b, and c are shown in each case.

levels and male sex were independent predictors for the presence of BrPh ECG in patients with severe hyperkalemia. 5. As shown by the response to adenosine infusion and computer simulations, ECG manifestations of systemic hyperkalemia are a consequence of the depolarized resting membrane potential and reduced sodium-channel availability for action potential activation, which results in delayed and heterogeneous conduction, or block, particularly in the presence of fibrosis at the RVOT.

Systemic Hyperkalemia Causing BrPh

Systemic hyperkalemia is most frequently found in patients with chronic and acute renal failure and/or concomitant treatments with nephrotoxic medications or K-sparing drugs. The classical electrocardiographic manifestations of hyperkalemia were first documented in the early 1950s by the presence of peaked T waves, shortened QT interval, lengthening of the PR interval, loss of *P* waves, and widening of the QRS complex.[28] Moreover, Levine et al also described the presence of the "dialyzable" current of injury resembling acute myocardial infarction or pericarditis.[29] However, Littmann et al reported the first consecutive series that recognized the similarities between the classic BrS ECG manifestations and those occasionally shown in the context of severe hyperkalemia.[11] In agreement with this and other studies,[10,11,30] we found that BrPh was most likely present in critically ill male patients with severe decompensation of their renal function and/or malignancies, with high mortality mostly related to their underlying clinical condition. In addition, we found that compared with hyperkalemic patients without Brugada ECG, the BrPh patients presented in males with higher serum K^+ values (1 mmol/L higher on average). Moreover, lower pH was also strongly related to the development of BrPh. These data, together with the presence of other outcome predictors, such as younger age, lower hypertension prevalence, and lesser chronic renal disease, further confirm the importance of acute increments in K^+ levels, which might be underestimated in terminal renal failure patients.[31] Given that the density of the strong inward rectifying K^+ current, I_{K1}, which maintains the resting membrane potential of the ventricular myocyte, is strictly controlled by $[K^+]_o$, acute increases in $[K^+]_o$, however transient, may place such patients at risk of malignant arrhythmias.[32] The findings of our multivariant analyses further support the predominant role of male sex and higher hyperkalemia levels, together with the role for the acid

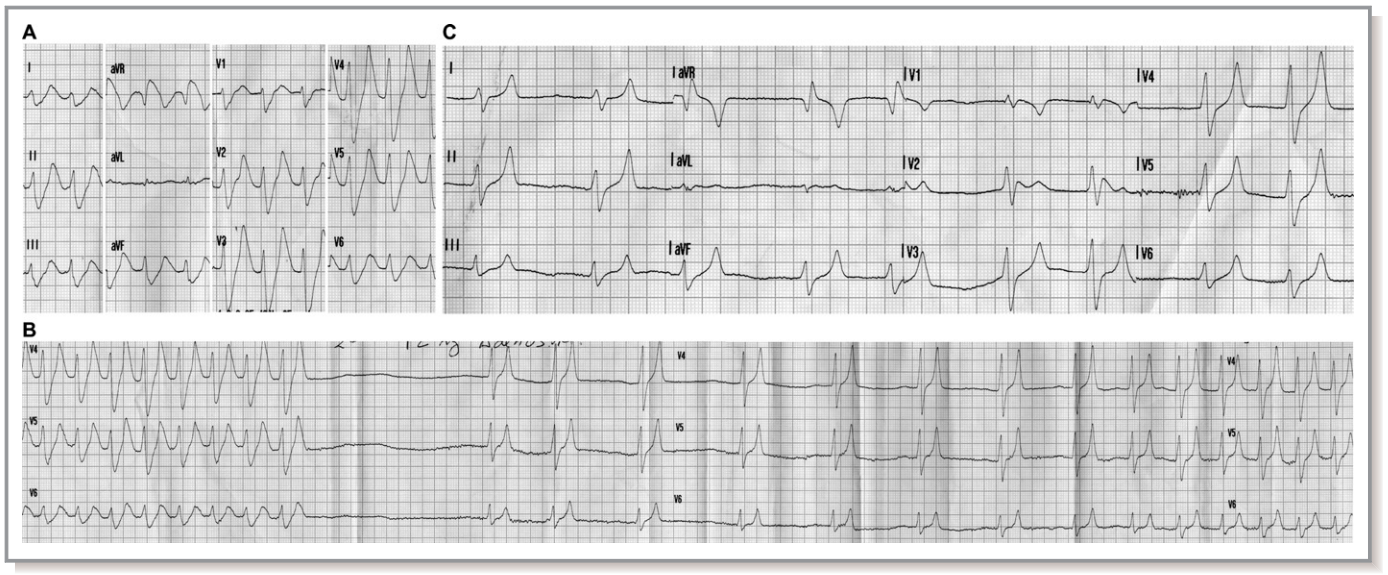

Figure 8. Wide complex tachycardia response to adenosine in a patient with severe hyperkalemia. **A**, Wide complex tachycardia upon arrival (serum potassium [K]=9.1 mmol/L). **B**, ECG recording during peak adenosine effect showing sinus arrest and significant QRS narrowing, followed by accelerated ventricular rhythm with progressive QRS widening later after disappearance of the adenosine effect. **C**, One hour later, after the initial treatment of hyperkalemia ([K] = 8.1 mmol/L).

group presence on the reduction of channel conductance favoring the occurrence of malignant ventricular arrhythmias, as shown in our simulations.[33]

We compared the clinical manifestations, ECG, and outcomes (malignant arrhythmias and mortality) of BrPh patients with those of severe hyperkalemic patients ($K^+ \geq 6.5$ mmol/L) without BrS phenotype. Overall, patients with the BrPh ECG had a grave prognosis with a short- to mid-term fatality rate of 51% not only related to the baseline clinical disease, but also to the clinical impact of malignant ventricular arrhythmias. Moreover, although patients presenting with BrPh had a higher likelihood of developing malignant arrhythmias than non-BrPh patients (43% versus 25%), in-hospital mortality was similar because of the poor clinical status in both groups. Junttila et al [34] reported on a series of patients with typical Brugada-type ECG during an acute medical event (including 5 patients with electrolyte imbalance), where 51% presented malignant arrhythmias and 38% developed sudden cardiac arrest. Unfortunately, in that report, only a minority of patients had a confirmed BrS genetic test. In our cohort of surviving patients, the characteristic BrS ECG changes disappeared when K^+ levels normalized. We attempted to perform a flecainide test after serum K^+ levels became normal and found a BrS typical ECG that was unmasked by the hyperkalemic state. Postema et al[35] previously reported a similar case of diabetic ketoacidosis with concomitant hyperkalemia that uncovered a typical BrS.

We compared the ECG of hyperkalemic patients and found that patients showing a BrPh had a wider QRS, and frequently presented abnormal QRS axis and a greater T-wave height compared with non-BrPh hyperkalemic patients (Table 3). This contrasted with patients with inheritable BrS that usually have mildly widened QRS complexes, but normal QRS axes on an otherwise normal ECG.[11,36] Thus, the presence of moderate-to-severe hyperkalemia, especially with a Brugada ECG pattern or atypical ST-segment elevation on the right precordial leads without BrS, should be aggressively treated and considered a risk factor for development of life-threatening cardiac arrhythmias. This is in agreement with previous studies showing that presence of an aVR sign and/or ST-segment elevation on the right precordial leads pattern reflects more right ventricular conduction delay and electrical heterogeneity, increasing the risk for developing arrhythmic events.[18,19]

Mechanism of Proarrhythmic Risk of BrPh Pattern Attributed to Hyperkalemia

To our knowledge, the relationship between hyperkalemia and the BrS ECG manifestations had not yet been systematically investigated. Together, the clinical results and computer simulations presented above provide mechanistic insight into the manifestation of electrolytic dysregulation causing Brugada phenotype. Even in the absence of genetic disease (eg, inheritable SCN5A mutations), delays in ventricular activation, and propagation failure at the RVOT, magnified by the presence of hyperkalemia and, possibly, low acid base state, promote the required electrophysiological changes, including APD shortening, membrane depolarization, and reduced sodium-channel availability, which enable the manifestation of BrPh ECG, an effect that is magnified by RVOT fibrosis. Introduction of

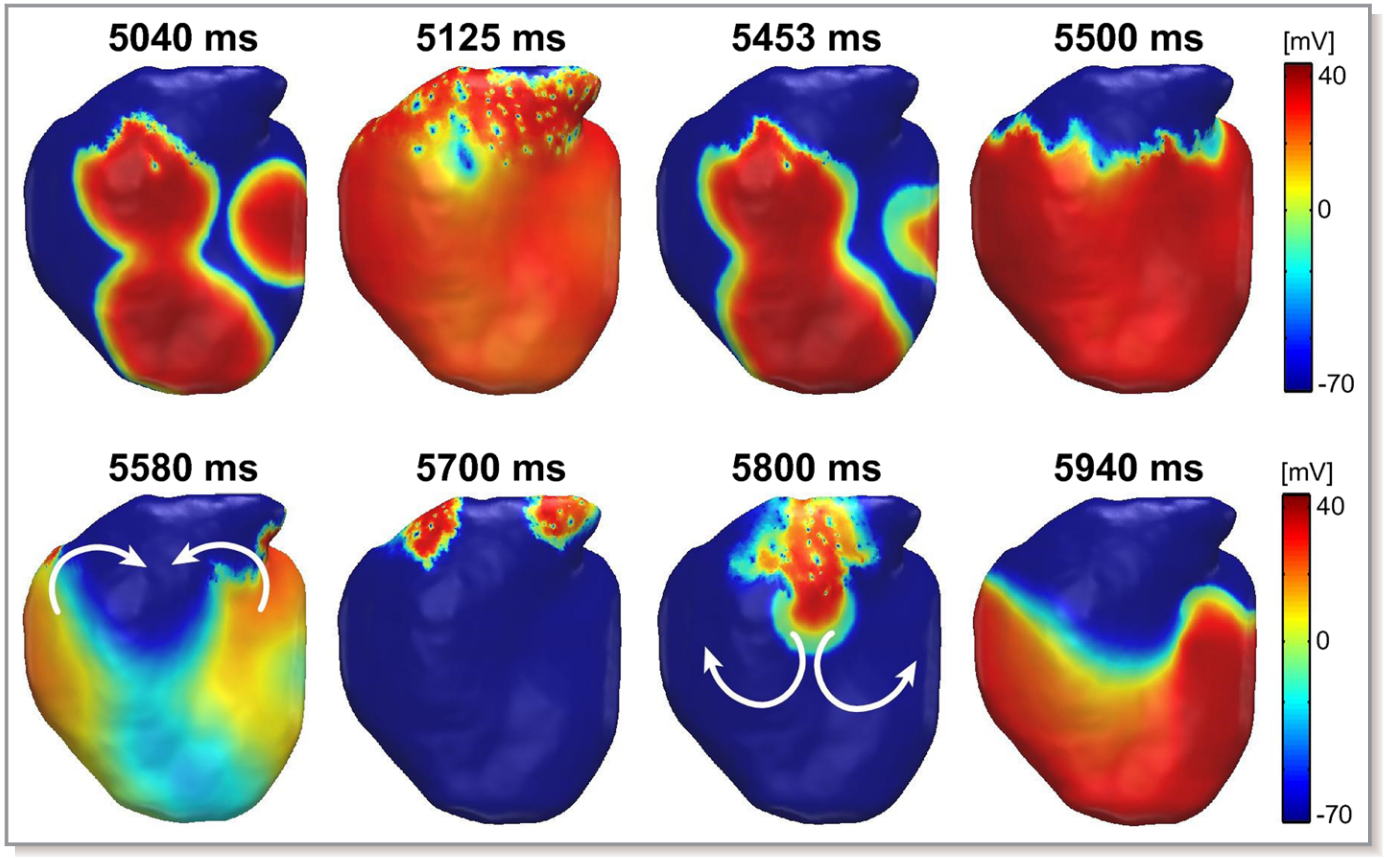

Figure 9. Monomorphic ventricular tachycardia induction during burst stimulation train followed by an extrastimuli at 400 ms allowed a stable reentry formation at the right ventricular outflow tract (RVOT) fibrotic site in a model with hyperkalemic conditions and extracellular potassium concentration of 10.0 mmol/L.

fibrotic tissue reduced the excitability of the RVOT and slowed CV, leading to a ST-segment elevation on V1 and V2 leads, creating the substrate for inducibility of malignant arrhythmias. In agreement with previous clinical reports, computer simulations showed that programmed stimulation caused electrogram fractionation and unidirectional block to initiate stable reentry formation without the need of an extrasytole.[8] Unexcitability attributed to the high concentration of potassium and its propensity to the generation of arrhythmias agrees with recent reports.[12] These results are supported by simulations by other groups showing that activation delay and right ventricular excitation failure attributed to current-load mismatch secondary to decrease in calcium current or increase in I_{to} can cause BrS.[16,17] Similar mechanisms could be responsible for other types of BrPh, with low availability of sodium channels given that it occurs during hypothermia or acidosis in ischemic regions.

The relative increase in I_{to} density at the RVOT reduced the need for slow conduction caused by hyperkalemia and resulted in spatial gradients of membrane voltage giving rise to the typical ST-segment elevation found in BrPh. In agreement with BrS, the strong sex-related predominance found in the BrPh indirectly supports the prominence of the transient outward current-mediated action potential notch in the right ventricular epicardium of males.[37] Moreover, the combination of abnormal repolarization and abnormal conduction not only explains the phenotypic manifestation of the BrPh, but also its clinical arrhythmic outcomes in the form of sustained ventricular reentrant patterns. On one hand, the presence of steep repolarization gradients causes asymmetry in excitability that gives rise to unidirectional block. On the other, slow conduction shortens the wavelength of the reentrant AP facilitating reentrant stabilization (Figures 8 and 9). Therefore, severe hyperkalemia leading to inactivation of the sodium channel in conjunction with presence of subtle structural abnormalities of the FVOT were responsible for the BrPh manifestation and reentrant arrhythmia occurrence in this setting.

Limitations

The observational and retrospective nature of the study prevented clinical data collections (ie, acid group value) and reduced the number of available ECGs. Although the computer simulations support the theory that RVOT has a major role producing Brugada patterns, further clinical data (histological and image data) and cellular studies are necessary to accurately define the substrate of this clinical entity in

this environment.[15,38] For example, imaging (eg, magnetic resonance imaging) data in patients presenting with a BrPh ECG could have shown enhanced fibrosis in the RVOT, as predicted by the modeling results. However, magnetic resonance imaging was nearly impossible in our study because of the fact that many of the patients were critically ill and had a very poor outcome, which substantially limited the number of patients available to study.

Conclusion

This report adds to our understanding of the electrocardiographic features of hyperkalemic BrPh patients. In patients with severe hyperkalemia attributed to critical medical conditions, a BrPh ECG is associated with a high prevalence of malignant arrhythmias and high all-cause mortality. BrPh ECG manifestations in patients with hyperkalemia are attributed to depolarized resting membrane potential and reduced availability of inward sodium channels. Although I_{to} elevation contributes, it is not essential to generate the hyperkalemic Brugada phenotype.

Sources of Funding

This work was funded in part by the CIBERCV (Centro de Investigacion Biomedica en Red Enfermedades Cardiovasculares), Instituto de Salud Carlos III (PI14/00857, DTS16/0160, PI17/1059, PI01106), Spanish Ministry of Ecomomy (TEC2013-46067-R) and the ERDF (European Regional Development Fund).

Disclosures

Dr Atienza is on the Advisory Board of Medtronic. Dr Jalife receives research funding from Abbott EP and Medtronic, Inc. The remaining authors have no disclosures to report.

References

1. Brugada P, Brugada J. Right bundle branch block, persistent ST segment elevation and sudden cardiac death: a distinct clinical and electrocardiographic syndrome: a multicenter report. *J Am Coll Cardiol*. 1992;20:1391–1396.
2. Antzelevitch C; Heart Rhythm Society; European Heart Rhythm Association. Brugada syndrome: report of the second consensus conference: endorsed by the Heart Rhythm Society and the European Heart Rhythm Association. *Circulation*. 2005;111:659–670.
3. Priori SG, Wilde AA, Horie M, Cho Y, Behr ER, Berul C, Blom N, Brugada J, Chiang C, Huikuri H. HRS/EHRA/APHRS expert consensus statement on the diagnosis and management of patients with inherited primary arrhythmia syndromes. *Heart Rhythm*. 2013;10:1932–1963.
4. Antzelevitch C, Yan GX, Ackerman MJ, Borggrefe M, Corrado D, Guo J, Gussak I, Hasdemir C, Horie M, Huikuri H, Ma C, Morita H, Nam GB, Sacher F, Shimizu W, Viskin S, Wilde AAM. J-Wave syndromes expert consensus conference report: emerging concepts and gaps in knowledge. *Europace*. 2017;19:665–694.
5. Bezzina CR, Barc J, Mizusawa Y, Remme CA, Gourraud J, Simonet F, Verkerk AO, Schwartz PJ, Crotti L, Dagradi F. Common variants at SCN5A-SCN10A and HEY2 are associated with Brugada syndrome, a rare disease with high risk of sudden cardiac death. *Nat Genet*. 2013;45:1044.
6. Frustaci A, Priori SG, Pieroni M, Chimenti C, Napolitano C, Rivolta I, Sanna T, Bellocci F, Russo MA. Cardiac histological substrate in patients with clinical phenotype of Brugada syndrome. *Circulation*. 2005;112:3680–3687.
7. Corrado D, Zorzi A, Cerrone M, Rigato I, Mongillo M, Bauce B, Delmar M. Relationship between arrhythmogenic right ventricular cardiomyopathy and Brugada syndrome: new insights from molecular biology and clinical implications. *Circ Arrhythm Electrophysiol*. 2016;9:e003631.
8. Coronel R, Casini S, Koopmann TT, Wilms-Schopman FJ, Verkerk AO, de Groot JR, Bhuiyan Z, Bezzina CR, Veldkamp MW, Linnenbank AC, van der Wal AC, Tan HL, Brugada P, Wilde AA, de Bakker JM. Right ventricular fibrosis and conduction delay in a patient with clinical signs of Brugada syndrome: a combined electrophysiological, genetic, histopathologic, and computational study. *Circulation*. 2005;112:2769–2777.
9. Probst V, Veltmann C, Eckardt L, Meregalli PG, Gaita F, Tan HL, Babuty D, Sacher F, Giustetto C, Schulze-Bahr E, Borggrefe M, Haissaguerre M, Mabo P, Le Marec H, Wolpert C, Wilde AA. Long-term prognosis of patients diagnosed with Brugada syndrome: results from the FINGER Brugada Syndrome Registry. *Circulation*. 2010;121:635–643.
10. Baranchuk A, Nguyen T, Ryu MH, Femenía F, Zareba W, Wilde AA, Shimizu W, Brugada P, Pérez-Riera AR. Brugada phenocopy: new terminology and proposed classification. *Ann Noninvasive Electrocardiol*. 2012;17:299–314.
11. Littmann L, Monroe MH, Taylor L, Brearley WD. The hyperkalemic Brugada sign. *J Electrocardiol*. 2007;40:53–59.
12. Weiss JN, Qu Z, Shivkumar K. Electrophysiology of hypokalemia and hyperkalemia. *Circ Arrhythm Electrophysiol*. 2017;10:e004667.
13. Wilde AA, Postema PG, Di Diego JM, Viskin S, Morita H, Fish JM, Antzelevitch C. The pathophysiological mechanism underlying Brugada syndrome: depolarization versus repolarization. *J Mol Cell Cardiol*. 2010;49:543–553.
14. Zhang J, Sacher F, Hoffmayer K, O'Hara T, Strom M, Cuculich P, Silva J, Cooper D, Faddis M, Hocini M, Haissaguerre M, Scheinman M, Rudy Y. Cardiac electrophysiological substrate underlying the ECG phenotype and electrogram abnormalities in Brugada syndrome patients. *Circulation*. 2015;131:1950–1959.
15. Nademanee K, Hocini M, Haïssaguerre M. Epicardial substrate ablation for Brugada syndrome. *Heart Rhythm*. 2017;14:457–461.
16. Hoogendijk MG, Opthof T, Postema PG, Wilde AA, de Bakker JM, Coronel R. The Brugada ECG pattern: a marker of channelopathy, structural heart disease, or neither? Toward a unifying mechanism of the Brugada syndrome. *Circ Arrhythm Electrophysiol*. 2010;3:283–290.
17. Hoogendijk MG, Potse M, Linnenbank AC, Verkerk AO, den Ruijter HM, van Amersfoorth SC, Klaver EC, Beekman L, Bezzina CR, Postema PG. Mechanism of right precordial ST-segment elevation in structural heart disease: excitation failure by current-to-load mismatch. *Heart Rhythm*. 2010;7:238–248.
18. Tsuneoka H, Takagi M, Murakoshi N, Yamagishi K, Yokoyama Y, Xu D, Sekiguchi Y, Yamasaki H, Naruse Y, Ito Y. Long-Term Prognosis of Brugada-Type ECG and ECG With Atypical ST-Segment Elevation in the Right Precordial Leads Over 20 Years: Results From the Circulatory Risk in Communities Study (CIRCS). *J Am Heart Assoc*. 2016;5:e002899. DOI: 10.1161/JAHA.115.002899.
19. Bigi MAB, Aslani A, Shahrzad S. aVR sign as a risk factor for life-threatening arrhythmic events in patients with Brugada syndrome. *Heart Rhythm*. 2007;4:1009–1012.
20. van Oosterom A, Oostendorp TF. ECGSIM: an interactive tool for studying the genesis of QRST waveforms. *Heart*. 2004;90:165–168.
21. O'Hara T, Virág L, Varró A, Rudy Y. Simulation of the undiseased human cardiac ventricular action potential: model formulation and experimental validation. *PLoS Comput Biol*. 2011;7:e1002061.
22. Dutta S, Mincholé A, Quinn TA, Rodriguez B. Electrophysiological properties of computational human ventricular cell action potential models under acute ischemic conditions. *Prog Biophys Mol Biol*. 2017;129:40–52.
23. Cardone-Noott L, Bueno-Orovio A, Mincholé A, Zemzemi N, Rodriguez B. Human ventricular activation sequence and the simulation of the electrocardiographic QRS complex and its variability in healthy and intraventricular block conditions. *EP Europace*. 2016;18:iv4–iv15.
24. Pelleg A, Mitamura H, Price R, Kaplinsky E, Menduke H, Dreifus LS, Michelson EL. Extracellular potassium ion dynamics and ventricular arrhythmias in the canine heart. *J Am Coll Cardiol*. 1989;13:941–950.
25. Giudicessi JR, Ye D, Tester DJ, Crotti L, Mugione A, Nesterenko VV, Albertson RM, Antzelevitch C, Schwartz PJ, Ackerman MJ. Transient outward current (I to) gain-of-function mutations in the KCND3-encoded Kv4. 3 potassium channel and Brugada syndrome. *Heart Rhythm*. 2011;8:1024–1032.
26. García-Molla VM, Liberos A, Vidal A, Guillem M, Millet J, Gonzalez A, Martínez-Zaldívar F, Climent AM. Adaptive step ODE algorithms for the 3D simulation of

electric heart activity with graphics processing units. *Comput Biol Med*. 2014;44:15–26.

27. Atienza F, Almendral J, Moreno J, Vaidyanathan R, Talkachou A, Kalifa J, Arenal A, Villacastin JP, Torrecilla EG, Sanchez A, Ploutz-Snyder R, Jalife J, Berenfeld O. Activation of inward rectifier potassium channels accelerates atrial fibrillation in humans: evidence for a reentrant mechanism. *Circulation*. 2006;114:2434–2442.
28. Ettinger PO, Regan TJ, Oldewurtel HA. Hyperkalemia, cardiac conduction, and the electrocardiogram: a review. *Am Heart J*. 1974;88:360–371.
29. Levine HD, Wanzer SH, Merrill JP. Dialyzable currents of injury in potassium intoxication resembling acute myocardial infarction or pericarditis. *Circulation*. 1956;13:29–36.
30. Anselm DD, Gottschalk BH, Baranchuk A. Brugada phenocopies: consideration of morphologic criteria and early findings from an international registry. *Can J Cardiol*. 2014;30:1511–1515.
31. Guo J, Massaeli H, Xu J, Jia Z, Wigle JT, Mesaeli N, Zhang S. Extracellular K+ concentration controls cell surface density of IKr in rabbit hearts and of the HERG channel in human cell lines. *J Clin Invest*. 2009;119:2745–2757.
32. Sakmann B, Trube G. Conductance properties of single inwardly rectifying potassium channels in ventricular cells from guinea-pig heart. *J Physiol*. 1984;347:641–657.
33. Bérubé J, Chahine M, Daleau P. Modulation of HERG potassium channel properties by external pH. *Pflügers Arch*. 1999;438:419–422.
34. Junttila MJ, Gonzalez M, Lizotte E, Benito B, Vernooy K, Sarkozy A, Huikuri HV, Brugada P, Brugada J, Brugada R. Induced Brugada-type electrocardiogram, a sign for imminent malignant arrhythmias. *Circulation*. 2008;117:1890–1893.
35. Postema PG, Vlaar AP, DeVries JH, Tan HL. Familial Brugada syndrome uncovered by hyperkalaemic diabetic ketoacidosis. *Europace*. 2011;13:1509–1510.
36. Smits JP, Eckardt L, Probst V, Bezzina CR, Schott JJ, Remme CA, Haverkamp W, Breithardt G, Escande D, Schulze-Bahr E. Genotype-phenotype relationship in Brugada syndrome: electrocardiographic features differentiate SCN5A-related patients from non-SCN5A-related patients. *J Am Coll Cardiol*. 2002;40:350–356.
37. Di Diego JM, Cordeiro JM, Goodrow RJ, Fish JM, Zygmunt AC, Perez GJ, Scornik FS, Antzelevitch C. Ionic and cellular basis for the predominance of the Brugada syndrome phenotype in males. *Circulation*. 2002;106:2004–2011.
38. Guillem MS, Climent AM, Millet J, Berne P, Ramos R, Brugada J, Brugada R. Spatiotemporal characteristics of QRS complexes enable the diagnosis of Brugada syndrome regardless of the appearance of a type 1 ECG. *J Cardiovasc Electrophysiol*. 2016;27:563–570.